Journal of Molecular Catalysis B: Enzymatic 61 (2009) 73–79

Contents lists available at ScienceDirect

Journal of Molecular Catalysis B: Enzymatic

journal homepage: www.elsevier.com/locate/molcatb

# Investigation of the carboligase activity of thiamine diphosphate-dependent enzymes using kinetic modeling and NMR spectroscopy

Mariya Kokova[a], Michael Zavrel[b], Kai Tittmann[c], Antje C. Spiess[b], Martina Pohl[a,*]

[a] Institute of Molecular Enzyme Technology, Heinrich-Heine University Düsseldorf, 52426 Jülich, Germany
[b] AVT–Biochemical Engineering, RWTH Aachen University, Worringerweg 1, D-52074 Aachen, Germany
[c] Albrecht-von-Haller-Institut, Georg-August-Universität Göttingen, Justus-von-Liebig-Weg 11, D-37077 Göttingen, Germany

ARTICLE INFO

*Article history:*
Available online 9 March 2009

*Keywords:*
Thiamine diphosphate-dependent enzymes
Kinetic modeling
NMR spectroscopy
Carboligation
Reaction mechanism
Intermediates

ABSTRACT

The benzoin condensation reaction catalyzed by the thiamine diphosphate (ThDP)-dependent enzymes benzaldehyde lyase (BAL) and benzoylformate decarboxylase variant His281Ala (BFD*H281A*) was studied via initial rate measurements, progress curve analysis and NMR-based analysis of reaction intermediates. Using a mechanistic kinetic model, the kinetic parameters and microscopic rate constants were determined, thus identifying the rate limiting steps of the reaction. In BAL, overall reaction is rate-limited by product release, whereas in BFD*H281A* substrate binding is the slowest step of catalysis. These results were further confirmed by analysis of covalent reaction intermediates using NMR spectroscopy after acid quench isolation.



## 1. Introduction

The benzoin condensation is a key C–C bond forming reaction between aromatic aldehydes, which is traditionally performed by chemical catalysts [1]. Alternatively, the reaction can be catalyzed by enzymes, especially when products of high enantiomeric purity are required. In that concern, the thiamine diphosphate (ThDP)-dependent enzymes benzaldehyde lyase and benzoylformate decarboxylase are successfully employed for chemo-enzymatic synthesis involving carboligation steps [2].

Benzaldehyde lyase (BAL, EC 4.1.2.38) from *Pseudomonas fluorescens Biovar I* has been first described by Gonzalez and Vicuna [3] as a thiamine diphosphate (ThDP)-dependent enzyme able to cleave the acyloin linkage of benzoin to yield two molecules of benzaldehyde. As the enzyme is strictly selective for conversion of the (*R*)-enantiomer, it can be applied in kinetic resolution of racemic benzoins [4,5]. Although BAL was initially described to show only lyase activity, it was later discovered that it can also catalyze the reverse reaction, that is the carboligation of benzaldehyde to (*R*)-benzoin with high enantiomeric excess (*ee*) > 99% [4,5]. Moreover, the enzyme has been demonstrated to catalyze formation of various highly enantiopure (*R*)-hydroxypropiophenone derivatives, using short-chain aliphatic aldehydes as acceptors and aromatic aldehydes including *ortho*-substituted ones as donor substrates [6].

Benzoylformate decarboxylase (BFD) (EC 4.1.1.7) from *Pseudomonas putida* was first reported by Wilcocks et al. [7]. The enzyme is involved in the non-oxidative decarboxylation of benzoylformate [8], and is moreover able to catalyze the enantioselective synthesis of (*S*)-2-hydroxypropanone derivatives as a side reaction [9]. BFD further catalyzes the ligation of a broad range of aromatic, heteroaromatic, conjugated olefinic aldehydes as donor substrates, preferably with acetaldehyde as an acceptor. Besides acetaldehyde, BFD converts aromatic and heteroaromatic substrates as acceptors to produce enantiopure (*R*)-benzoin and derivatives thereof, but in contrast to BAL with very low reaction rates [8]. The benzoin-forming activity of BFD was enhanced by site-directed mutagenesis of histidine 281 to alanine, yielding more space in the active site for accommodating larger acceptor aldehydes [9]. Therefore, the variant BFD*H281A* was chosen together with wild-type BAL for our research purposes.

A severe technical problem is the low solubility of the benzoin substrates in aqueous buffer. Addition of 20–30% DMSO in the reaction mixture considerably improves the solubility of the substrates, and thus the enzymatic performance [10]. Both BAL and BFD are known to catalyze the benzoin formation from two benzaldehyde molecules enantioselectively (more than 99% *ee*) and high conversion (BAL 97% and BFD 70%, in the presence of DMSO) [9]. However, the effect of organic solvents on the stability and activity of these enzymes has not been characterized in detail.

The catalytic cycle of the reaction catalyzed by BAL [4] can be subdivided into three main steps (Scheme 1). At first, the

* Corresponding author at: Institute of Molecular Enzyme Technology, Heinrich-Heine Universität Düsseldorf, Research Center Jülich, 52426 Jülich, Germany.
Tel.: +49 2461 613704; fax: +49 2461 612490.
*E-mail address:* ma.pohl@fz-juelich.de (M. Pohl).

1381-1177/$ – see front matter © 2009 Elsevier B.V. All rights reserved.
doi:10.1016/j.molcatb.2009.02.021

**Nomenclature**

| | |
|---|---|
| BAL | Benzaldehyde lyase |
| BFD | Benzoylformate decarboxylase |
| ThDP | Thiamine diphosphate |
| Hbz-ThDP | Hydroxybenzyl-thiamine diphosphate intermediate |
| Benzoin-ThDP | Benzoin-thiamine diphosphate intermediate |
| BSA | Bovine serum albumin |
| DMSO | Dimethyl sulfoxide |
| TCA | Trichloroacetic acid |
| $A$ | concentration of first binding substrate (mM) |
| $k$ | microscopic rate constant ($s^{-1}$), ($mM^{-1}\,s^{-1}$) |
| $K_{catf}$ | maximum turnover number ($s^{-1}$) |
| $K_{eq}$ | equilibrium constant ($mM^{-1}$) |
| $K_{iA}$ | inhibition constant of the first binding substrate (mM) |
| $K_{iB}$ | inhibition constant of the second binding substrate (mM) |
| $K_{mA}$ | Michaelis constant for the first binding substrate (mM) |
| $K_{mB}$ | Michaelis constant for the second binding substrate (mM) |
| $K_{mP}$ | Michaelis constant for the product (mM) |

reactive ylide form of ThDP binds a benzaldehyde molecule to form the first covalent intermediate: hydroxybenzyl-ThDP (HBz-ThDP) (step 1). After deprotonation of C2α, a highly reactive nucleophilic enamine-carbanion intermediate is formed, which adds to the second benzaldehyde molecule to yield benzoin-ThDP (step 2). Finally, (*R*)-benzoin is released from that adduct and the cofactor is regenerated (step 3). The protonation step can be considered to occur very fast.

The benzoin condensation is a typical C–C bond forming reaction in which one molecule of benzaldehyde is the donor and the other is the acceptor substrate [11]. So far, the donor–acceptor concept has been considered only for two different substrates. By varying the concentration of one respective substrate, their Michaelis constants ($K_{mA}$ and $K_{mB}$) can be determined. Up to now, only one apparent $K_m$ value has been assumed, if one substrate is both a donor and acceptor [10,12]. Recently, a mechanistic kinetic model has been derived which can estimate kinetic parameters using progress curve analysis by monitoring the substrate decrease or the product increase over time. The model can estimate the maximum turnover number for the forward reaction $k_{catf}$, the thermodynamic equilibrium constant $K_{eq}$ for the overall reaction and the Michaelis constants for the donor and the acceptor ($K_{mA}$ and $K_{mB}$), even in case the molecules are identical. Moreover, the dependent parameters ($K_{iA}$, $K_{iB}$, and $K_{mP}$) can be calculated by using the given equations (Eqs. (2)–(4)). Since this kinetic model is mechanistic, the microscopic rate constants for every reaction step ($k_1$, $k_{-1}$, $k_2$, $k_{-2}$, $k_3$ and $k_{-3}$) can be calculated with very good accuracy. The results for the synthesis of (*R*)-3,3′,5,5′-tetramethoxybenzoin using BAL implicated the product release to be rate-limiting [13].

In this contribution, the benzoin condensation catalyzed by both BAL and BFD*H281A* were studied using a combined experimental and theoretical approach. At first, initial rate measurements were performed. Moreover, the above described mechanistic kinetic model was applied to determine the catalytic parameters by progress curve analysis. Finally, steady-state intermediate analysis

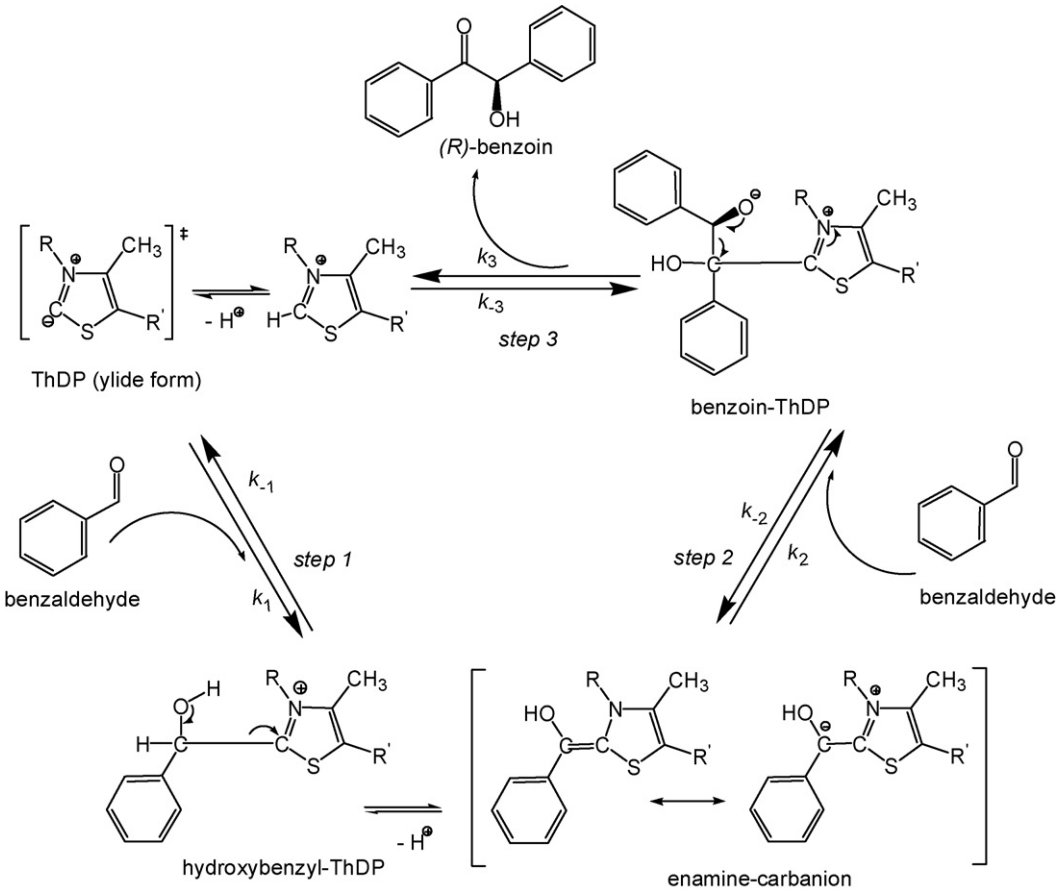


**Scheme 1.** Mechanism of BAL and BFD-catalyzed benzoin formation.

by $^1$H NMR was performed for a detailed study of the microscopic reaction steps [14]. Accordingly, the catalytic parameters were determined and the rate-limiting steps of the reaction identified. Also, the effects of the cosolvents acetone and DMSO on the reaction kinetics and mechanism were analyzed.

## 2. Experimental

### 2.1. Chemicals

All reagents and organic solvents including deuterated acetone and DMSO were purchased from Sigma Aldrich; and the buffering salts were from Roth. All chemicals were of analytical purity.

### 2.2. Initial rate measurements

The initial rate measurements were conducted by quantifying the benzoin formation from benzaldehyde within the first minute. The reaction mixture consisted of benzaldehyde (5–60 mM) in potassium phosphate buffer (50 mM), containing 2.5 mM $MgSO_4$, 0.5 mM ThDP and BAL (5–10 μg/ml) or BFD*H281A* (40–60 μg/ml). BAL kinetics was studied at pH 8 and in case of BFD*H281A* at pH 6.5. The assay temperature for both enzymes was kept at 30 °C. To measure the amount of formed benzoin, samples were taken at appropriate time intervals, diluted in acetonitrile (1:20) to inactivate the enzyme, centrifuged and subjected to HPLC analysis (Gynkotek), equipped with an ODS Multohyp column (5μ, CS-Chromatographie, Germany) and a UV-detector. The experiments were also conducted in the presence of cosolvents. Activity of BAL was measured in 10 vol% DMSO and 20 vol% acetone, activity of BFD*H281A* was additionally studied in 20 vol% DMSO.

Initial rate velocities refer to one monomer of the tetrameric enzymes.

The protein content was determined according to Bradford [15] and using BSA as a standard.

### 2.3. Progress curve analysis

The kinetic data derived from the experiments described above were further used for progress curve analysis. In contrast to the initial rate measurements, up to seven samples were taken in order to follow the reaction within the first five minutes. The obtained data points for both benzaldehyde and benzoin were used to fit the mechanistic kinetic model (Eq. (1)) described in detail in [13]. Thereafter, the software package gPROMS (version 3.1.3) from Process Systems Enterprises Ltd. (London, UK) was applied for analysis. As demonstrated in [13], a model simplification is necessary in order to achieve precise and reliable parameter estimates. Thus, the microscopic rate constants $k_1$ and $k_2$, as well as $k_{-1}$ and $k_{-2}$ were considered to be identical, although this assumption needs further experimental confirmation.

$$v = -\frac{1}{2}\cdot\frac{dA}{dt} = \frac{(k_{catf}/K_{iA}\cdot K_{mB})\cdot(A^2-(P/K_{eq}))}{1+(A/K_{iA})(1+(K_{mA}/K_{mB}))+(A^2/K_{iA}\cdot K_{mB})+(P/K_{mP})+(A\cdot P/K_{mP}\cdot K_{iB})} \quad (1)$$

The dependent kinetic parameters were calculated according to Eqs. (2)–(4).

$$K_{iA} = K_{mB} - K_{mA} \quad (2)$$

$$K_{mP} = \frac{K_{mB}\cdot(K_{mB}-K_{mA})^2\cdot K_{eq}}{2\cdot K_{mA}} \quad (3)$$

$$K_{iB} = \frac{K_{mB}\cdot K_{iA}}{K_{mA}\cdot[1-((K_{mA}/K_{iA})-1)\cdot(K_{mP}/K_{eq}\cdot K_{mB}\cdot K_{iA})]} \quad (4)$$

To reduce the number of degrees of freedom the model parameter $K_{eq}$ was determined separately by averaging all equilibrium data. Based on the estimated values for the independent parameters $k_{catf}$, $K_{mA}$, and, $K_{mB}$ the microscopic rate constants were calculated using Eqs. (5)–(8):

$$k_1 = k_2 = \frac{k_{catf}}{K_{mA}} \quad (5)$$

$$k_{-1} = k_{-2} = \frac{k_{catf}\cdot(K_{mB}-K_{mA})}{K_{mA}} \quad (6)$$

$$k_3 = k_{catf} \quad (7)$$

$$k_{-3} = \frac{k_{catf}}{K_{eq}\cdot(K_{mB}-K_{mA})^2} \quad (8)$$

### 2.4. $^1$H NMR spectroscopy

Using a combined acid quench/$^1$H NMR-method, the relative distribution of ThDP and of the acid-stable intermediates HBz-ThDP and benzoin-ThDP can be assessed. Bases in these data, the net rate constants of the three main reaction steps can be estimated [14]. At first, the enzymes were repeatedly washed (three times) with 50 mM potassium phosphate buffer at 4 °C to remove excess ThDP. Thereafter, BAL (6 mg/ml) or BFD*H281A* (10 mg/ml) were mixed with 20 mM benzaldehyde in 50 mM potassium phosphate buffer (pH 7.5 for BAL and pH 6.5 for BFD*H281A*) at 30 °C for 1–2 s to assure steady-state conditions. The reactions were then stopped by addition of TCA/HCl [14]. Subsequently, the precipitated protein was discarded after centrifugation and the supernatant containing the intermediates, substrates and products of the reaction were subjected to 1D $^1$H NMR spectroscopy at 298 K and using water presaturation techniques for suppressing the water signal. For assignment and quantitative analysis of ThDP, HBz-ThDP and benzoin-ThDP, the 2′-$CH_3$ and 4-$CH_3$ $^1$H NMR singlet signals of ThDP (2.65 and 2.58 ppm), HBz-ThDP (2.47 and 2.42 ppm) and benzoin-ThDP (2.45 and 2.43 ppm) were used. NMR acquisition and data processing were essentially carried out as described previously [14].

## 3. Results and discussion

### 3.1. Initial rate measurements

With BAL, the direct $v_0$–[*S*] plots showed a hyperbolic increase approximately up to the respective limit of solubility of benzaldehyde (Fig. 1). The addition of DMSO and acetone improved the solubility of benzaldehyde, which is 35 mM in buffer, 79 mM in 10 vol% DMSO, 113 mM in 20 vol% DMSO, and 179 mM in 20 vol% acetone at room temperature. In buffer and in 10 vol% DMSO, the enzyme was inhibited at higher concentrations of benzaldehyde evidenced by the appearance of a second phase. Only in 20 vol% acetone this inhibition started below the solubility limit. Moreover, addition of the cosolvents accelerated the reaction rate at standard conditions (20 mM benzaldehyde). The reaction rate of BAL with 20 mM benzaldehyde amounts for 19.6 $s^{-1}$ (in buffer), 51.2 $s^{-1}$ (in 10 vol% DMSO) and 23.5 $s^{-1}$ (in 20 vol% acetone).

Interestingly, the $v_0$–[*S*] plots of BFD*H281A* showed only a linear increase until ~50 mM benzaldehyde indicating that the maximum reaction rate had not been achieved. Under standard reaction conditions (20 mM benzaldehyde), the substrate is by far not saturating (Fig. 1). Compared to BAL, BFD*H281A* was less sensitive to inactivation phenomena. At higher concentrations, the enzyme was inhibited only in buffer.

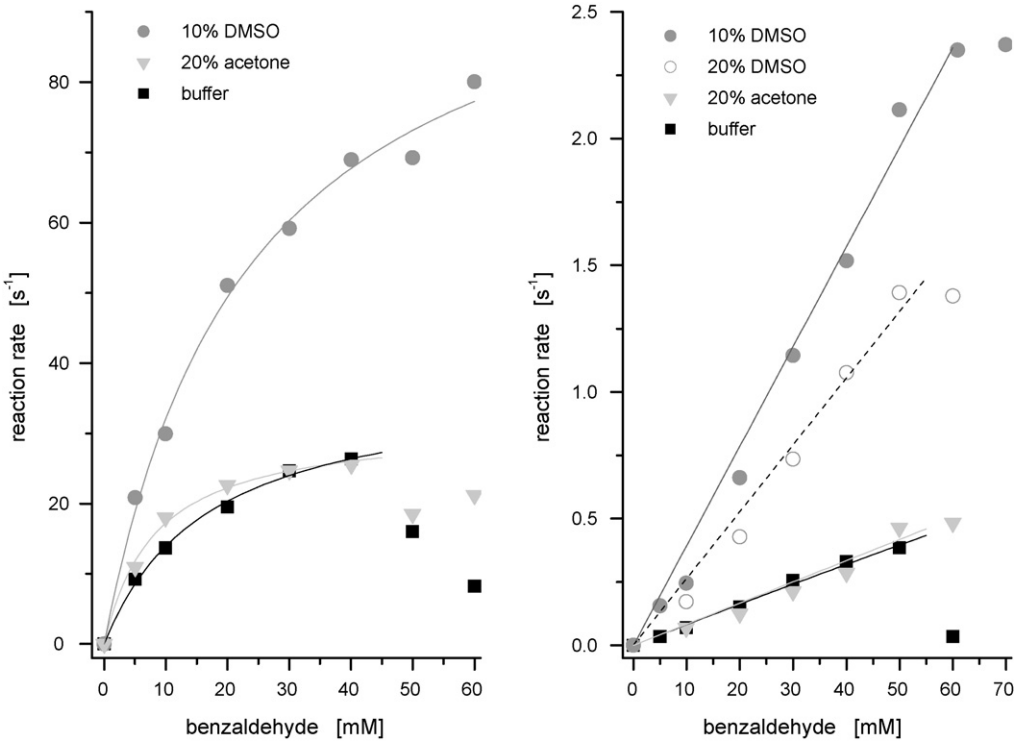


**Fig. 1.** Dependence of the catalytic activity of BAL and BFD*H281A* on the substrate concentration.

**Table 1**
Estimated independent parameters for the formation of benzoin from benzaldehyde in 50 mM potassium phosphate buffer plus added organic solvents.

| Enzyme | Organic solvent | $K_{eq}$ (mM$^{-1}$) | $k_{catf}$ (s$^{-1}$) | $K_{mA}$ (mM) | $K_{mB}$ (mM) |
|---|---|---|---|---|---|
| BAL | – | 3.019 | 35.1 ± 0.4 | 0.28 ± 0.05 | 0.39 ± 0.06 |
| | 10 vol% DMSO | 3.019 | 78.1 ± 0.9 | 1.96 ± 0.55 | 6.13 ± 0.08 |
| | 20 vol% acetone | 3.019 | 39.9 ± 0.6 | 1.47 ± 0.12 | 1.47 ± 0.12 |
| BFD*H281A* | – | 3.019 | 3.5 ± 0.5 | 131.3 ± 23.9 | 139.5 ± 23.1 |
| | 10 vol% DMSO | 3.019 | 11.7 ± 0.6 | 86.5 ± 8.5 | 109.5 ± 7.4 |
| | 20 vol% DMSO | 3.019 | 16.8 ± 2.6 | 234.3 ± 42.0 | 242.4 ± 42.0 |
| | 20 vol% acetone | 3.019 | 2.4 ± 0.4 | 42.5 ± 22.6 | 82.2 ± 18.8 |

The reaction rate of BFD*H281A* in buffer with 20 mM benzaldehyde was 0.17 s$^{-1}$, which is about two orders of magnitude lower than that of BAL. However, the addition of DMSO to the reaction mixture caused a similar effect: it significantly improved the reaction rate to 0.74 s$^{-1}$ and 0.48 s$^{-1}$ in the presence of 10 and 20 vol% DMSO, respectively. The reaction rate in 20 vol% acetone was estimated to be 0.14 s$^{-1}$.

### 3.2. Estimation of kinetic parameters from progress curve analysis

The obtained progress curves were fitted by the mechanistic kinetic model (Fig. 2). $K_{eq}$ was determined separately to equal 3.019 mM$^{-1}$. The obtained parameter estimates together with their standard deviations are listed in Table 1. It demonstrates that the maximum turnover number $k_{catf}$ can be estimated very precisely. The precision for $K_{mA}$ and $K_{mB}$ is also satisfactory. Apparently, the cosolvents affect all parameters, although their strongest impact is on $k_{catf}$. Both enzymes show a higher $k_{catf}$ in presence of the cosolvent compared to buffer with only one exception: BFD*H281A* in 20 vol% acetone. The strongest effect on both enzymes caused the addition of 10 vol% DMSO.

By comparison of the values obtained for both enzymes, it becomes apparent that BAL is about one order of magnitude more active than is BFD*H281A*. This is not surprising since BAL is known to be significantly more active concerning benzoin formation [9]. With only one exception (BAL in 20 vol% acetone), the $K_{mB}$-values are higher than $K_{mA}$ (Table 1). Compared to BAL, the $K_{mA}$ and $K_{mB}$ values of BFD*H281A* are huge, which was previously also described for wild-type BFD and propanal as a substrate [16]. This extremely low affinity for aliphatic or aromatic aldehyde substrates is probably a specific property of BFD.

The calculated dependent parameters are presented in Table 2. Obviously, the solvents affect also the inhibitory constants for substrate and product ($K_{iA}$ and $K_{iB}$) and the Michaelis constant of the product ($K_{mP}$). Once again, DMSO proved to be the better cosolvent (at 10 vol% concentration). Due to instability of BFD*H281A* in 20 vol% acetone, the parameters differ to some degree but still exhibit the same tendency.

**Table 2**
Calculated dependent parameters.

| Enzyme | Organic solvent | $K_{iA}$ (mM) | $K_{mP}$ (mM) | $K_{iB}$ (mM) |
|---|---|---|---|---|
| BAL | – | 0.11 | 0.02 | 0.22 |
| | 10 vol% DMSO | 4.18 | 82.62 | 8.36 |
| | 20 vol% acetone | 0.15 | 0.04 | 0.30 |
| BFD*H281A* | – | 8.19 | 107.58 | 16.38 |
| | 10 vol% DMSO | 23.00 | 1011.19 | 46.01 |
| | 20 vol% DMSO | 8.17 | 104.18 | 16.33 |
| | 20 vol% acetone | 39.76 | 4620.28 | 79.51 |

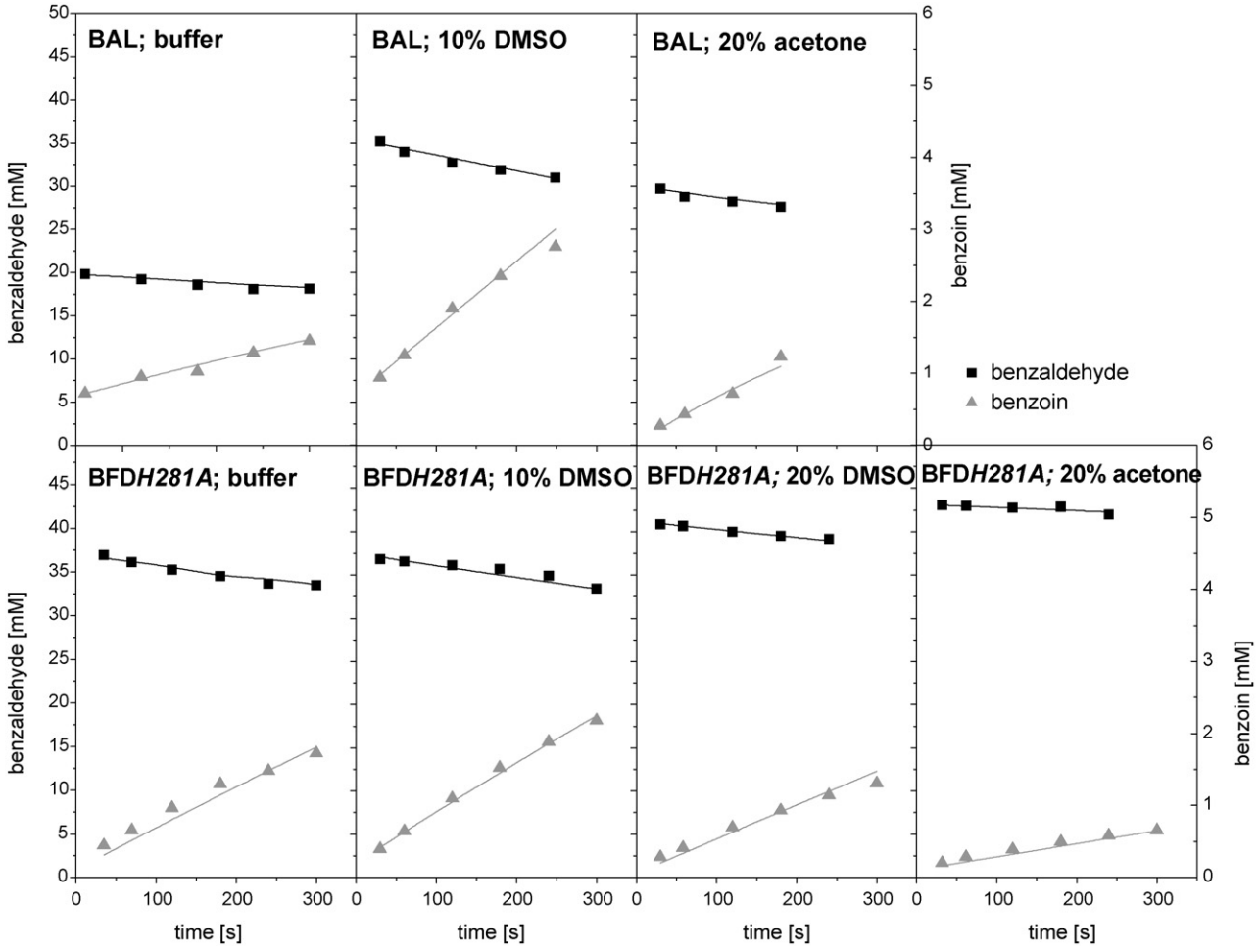


**Fig. 2.** Selection of progress curves fitted by the mechanistic kinetic model Eq. (1).

The microscopic rate constants (Fig. 3) were calculated according Eqs. (5)–(8). In this figure the calculated values are not only presented as numbers, but are also visualized in terms of a bar chart. Thus, it can be clearly seen that for BAL and the BFD variant different kinds of kinetic limitations exist. Catalysis of BAL is mostly rate-determined by product release. Moreover, the bar charts clearly visualize the kinetic effect of the cosolvents: they accelerate the release of benzoin, while they decrease the substrate binding rate. However, the overall reaction rate is increased since the product release is the bottleneck. Taking into account that $k_1$ and $k_2$ are second order rate constants, it may be concluded that above 2 mM substrate concentration the product release is always rate-limiting.

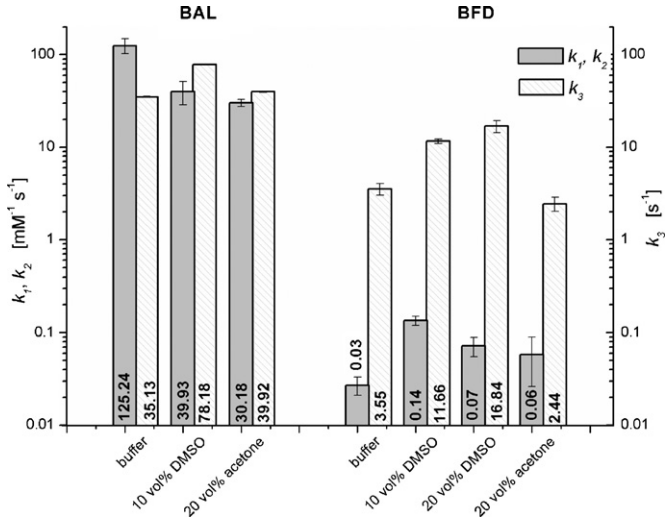


**Fig. 3.** Calculated microscopic rate constants. The constants $k_1$ and $k_2$ were considered to be identical.

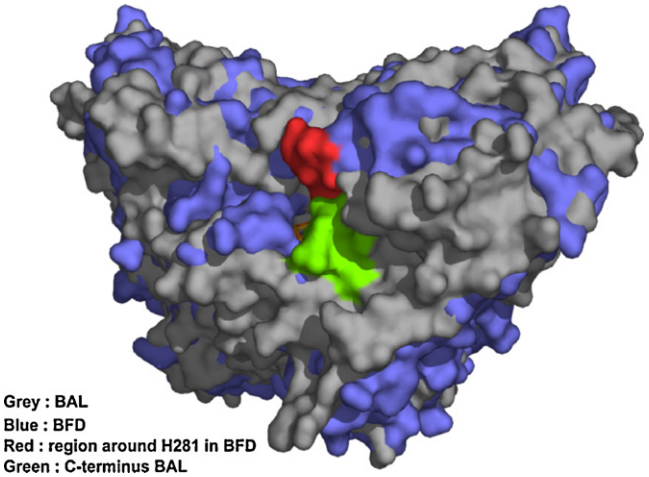


**Fig. 4.** Surface representation of BAL and BFD dimers: Grey: BAL; blue: BFD; Red: region around H281 in BFD; green: C-terminus BAL. The picture was generated by Dr. Michael Knoll based in the pdb entries 1mcz (BFD) and 2ag0 (BAL). The surfaces of the structures were visualized with the PyMol program (Version 0.98) [19].

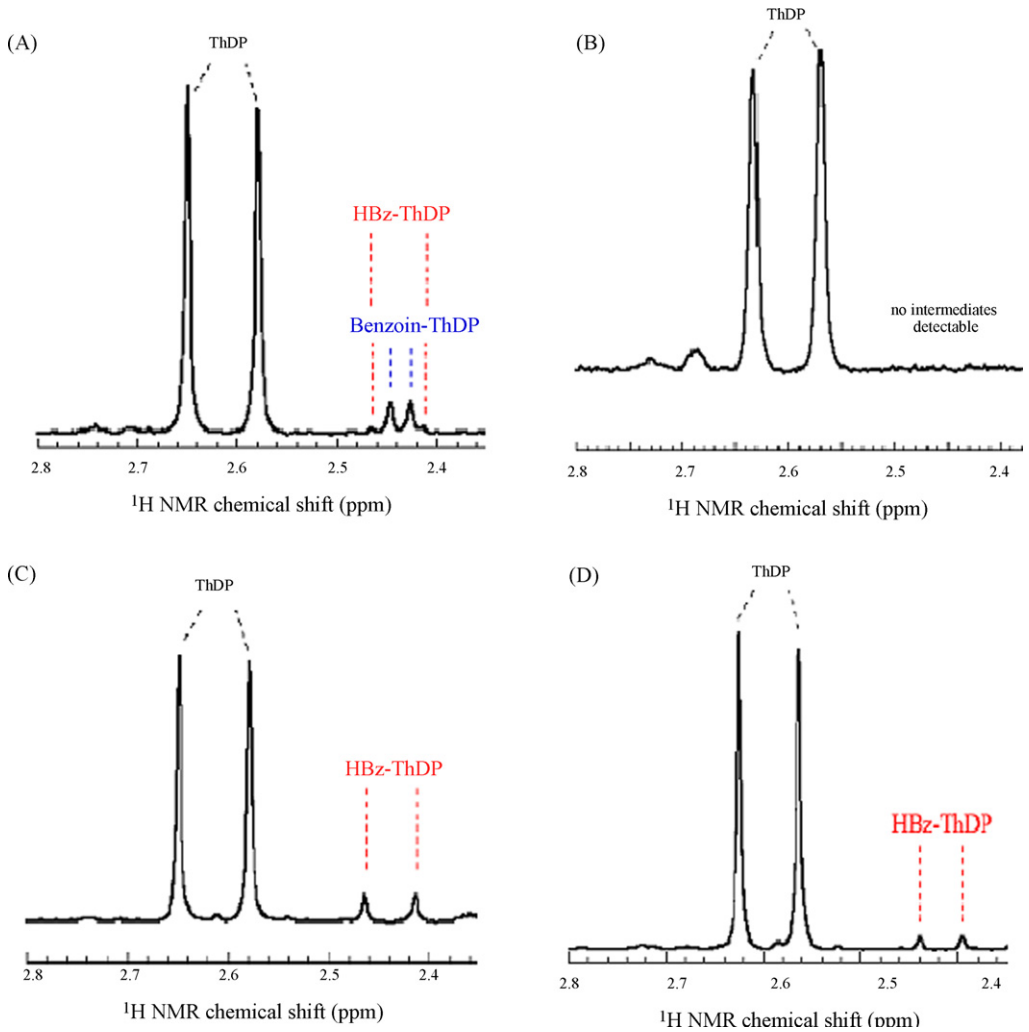


**Fig. 5.** Distribution of reaction intermediates from steady-state intermediate analysis by $^1$H NMR. The 2′-$CH_3$ and the 4-$CH_3$ fingerprint region is shown. (A) BAL in aqueous buffer; (B) BAL in 20 vol% acetone; (C) BFD*H281A* in aqueous buffer; (D) BFD*H281A* in 20 vol% acetone.

The same situation holds true in 10 vol% DMSO. These results are in line with recently reported data. For the synthesis of (*R*)-3,3′,5,5′-tetramethoxy benzoin catalyzed by BAL this was detected by using a mechanistic kinetic model [13]. Moreover, CD spectroscopic data indicated that the release of benzoin could be rate-limiting for BAL-catalyzed benzoin synthesis [17].

In contrast to this, the product release is the fastest reaction step for the benzoin formation catalyzed by BFD*H281A*, whereas the carboligation (step 2, Scheme 1) was identified as the rate-limiting step. The results clearly implicated DMSO to be a better cosolvent as compared to acetone, as all micro-reaction constants were increased in DMSO but decreased in acetone.

The different rate limitations with BAL and BFD*H281A* can be rationalized in terms of different active site geometries. Structural studies show that the active site of BAL is partly covered by a C-terminal helix (Fig. 4), which could hinder product release. In BFD such a structural element is absent, which might allow faster product release. Moreover, the active site pocket of BFD is smaller than that of BAL and the benzoin molecule could experience steric stress [18], which would enforce it to leave the active site all immediately after its formation.

### 3.3. Steady-state intermediate analysis by $^1$H NMR

To test the reliability of the progress curve analysis, a steady-state intermediate analysis employing $^1$H NMR spectroscopy as an analytic tool was carried out. When BAL was reacted with benzaldehyde without any cosolvent, all major intermediates (ThDP, HBz-ThDP, benzoin-ThDP) were identifiable in the NMR spectra (Fig. 5A). The amount of benzoin-ThDP was higher than that of HBz-ThDP, confirming that the release of benzoin is the rate-limiting step. In the presence of 20 vol% acetone, only C2-unsubstituted ThDP was detectable indicating that the product release is accelerated as already suggested by the progress curve analysis (Fig. 5B).

Using the established method detailed in [14], individual net rate constants can be calculated on the basis of the proton signal integrals of ThDP and of derived intermediates. However, in the current study, these results are treated as qualitative for two main reasons: first of all, the $v_0$–[*S*] plot (Fig. 1) shows that, owing to limited solubility of the substrate, $V_{max}$ was not achieved under the reaction conditions used (20 mM benzaldehyde). Secondly, it was observed that BAL rapidly loses the cofactor ThDP from the active sites when dissolved in buffer without excess cofactors. Unfortunately, the NMR analysis cannot distinguish between free and enzyme-bound ThDP thus making a quantitative estimation of enzyme-bound C2-unsubstituted ThDP not reliable.

Unlike BAL, BFD*H281A* did not lose ThDP in buffer without excess cofactors under the applied conditions. In this case, the high concentrations of C2-unsubstituted ThDP quantified by NMR were caused only by nonsaturation of the enzyme as a consequence of the extremely high $K_m$ values as discussed above. The $v_0$–[*S*] plot (Fig. 1) shows an almost linear increase up to the solubility limit

and no hyperbolic dependence is observable; therefore, the active sites were not saturated at the chosen reaction conditions (20 mM benzaldehyde).

Quantitative $^{1}$H NMR analysis of intermediates formed in the course of BFD*H281A*-catalyzed synthesis of benzoin revealed that in all cases only ThDP and HBz-ThDP were accumulated at steady-state (Fig. 5C + D), clearly indicating that carboligation (that is the addition of the second molecule benzaldehyde to HBz-ThDP) is rate-determining for the overall reaction. Addition of cosolvent (10, 20 vol% DMSO and 20 vol% acetone) slightly accelerates carboligation relative to HBz-ThDP formation but still the carboligation is rate-limiting. The product release is the fastest elementary reaction step as no benzoin-ThDP adduct could be observed, so once the benzoin-ThDP molecules are being formed, the product will immediately split off from ThDP. As stated before, these results are in good agreement with the results obtained by the progress curve analysis.

## 4. Conclusions

In this contribution it could be demonstrated that by conducting progress curve analysis with an appropriate mechanistic kinetic model, it is possible to determine the microscopic rate constants and the rate-limiting steps of benzoin condensation catalyzed by BAL and the BFD variant BFD*H281A*. The accuracy of the approach was experimentally supported by independent qualitative NMR-based analysis of on-pathway reaction intermediates. The model-based experimental analysis revealed that BAL is mainly limited by the product release, which is consistent with previous results [13,17]. For BFD*H281A*, the rate-limiting step has been identified to be carboligation of HBz-ThDP and benzaldehyde. To our knowledge, this is the first report succeeding in the identification of rate-limiting steps for carboligation catalyzed by a BFD variant.

## Acknowledgements

We thank Dr. Michael Knoll from the Institute of Technical Biochemistry, University of Stuttgart, for generating the surface presentations in Fig. 4. This work was financed in frame of the International Research Training Group "Biocatalysis in non-conventional solvents—Bionoco" (GK 1166).

## References

[1] T. Dudding, K.N. Houk, Proc. Natl. Acad. Sci. U.S.A. 101 (2004) 5770–5775.
[2] M. Pohl, B. Lingen, M. Müller, Chem. Eur. J. 8 (2002) 5288–5295.
[3] B. Gonzalez, R. Vicuna, J. Bacteriol. 171 (1989) 2401–2405.
[4] A.S. Demir, M. Pohl, E. Janzen, M. Müller, J. Chem. Soc. Perkin Trans. 1 (2001) 633–635.
[5] E. Janzen, M. Müller, D. Kolter-Jung, M.M. Kneen, M.J. McLeish, M. Pohl, Bioorg. Chem. 34 (2006) 345–361.
[6] A.S. Demir, Ö. Şeşenoglu, P. Dünkelmann, M. Müller, Org. Lett. 5 (2003) 2047–2050.
[7] R. Wilcocks, O.P. Ward, S. Collins, N.J. Dewdney, Y. Hong, E. Prosen, Appl. Environ. Microbiol. 58 (1992) 1699–1704.
[8] H. Iding, T. Dünnwald, L. Greiner, A. Liese, M. Müller, P. Siegert, J. Grötzinger, A.S. Demir, M. Pohl, Chem. Eur. J. 6 (2000) 1483–1495.
[9] A.S. Demir, T. Dünnwald, H. Iding, M. Pohl, M. Müller, Tetrahedron: Asymmetr. 10 (1999) 4769–4774.
[10] T. Stillger, M. Pohl, C. Wandrey, A. Liese, Org. Proc. Res. Dev. 10 (2006) 1172–1177.
[11] P. Dünkelmann, D. Kolter-Jung, A. Nitsche, A.S. Demir, P. Siegert, B. Lingen, M. Baumann, M. Pohl, M. Müller, J. Am. Chem. Soc. 124 (2002) 12084–12085.
[12] F. Hildebrand, S. Kühl, M. Pohl, D. Vasic-Racki, M. Müller, C. Wandrey, S. Lütz, Biotechnol. Bioeng. 96 (2007) 835–843.
[13] M. Zavrel, T. Schmidt, C. Mickalik, M. Ansorge-Schumacher, W. Marquardt, J. Büchs, A.C. Spiess, Biotechnol. Bioeng. 101 (2008) 27–38.
[14] K. Tittmann, R. Golbik, K. Uhlemann, L. Khailova, G. Schneider, M. Patel, F. Jordan, D.M. Chipman, R.G. Duggleby, G. Hübner, Biochemistry 42 (2003) 7885–7891.
[15] M.M. Bradford, Anal. Biochem. 72 (1976) 248–254.
[16] R. Mikolajek, A.C. Spiess, M. Pohl, S. Lamare, J. Büchs, ChemBioChem. 8 (2007) 1063–1070.
[17] S. Chakraborty, N. Nemeria, A. Yep, M. McLeish, G.L. Kenyon, F. Jordan, Biochemistry 47 (2008) 3800–3809.
[18] M. Knoll, M. Müller, P. Pleiss, M. Pohl, ChemBioChem. 7 (2006) 1928–1934.
[19] W.L. DeLano, The PyMOL Molecular Graphics System, http://www.pymol.org, San Carlo, CA, 2002.